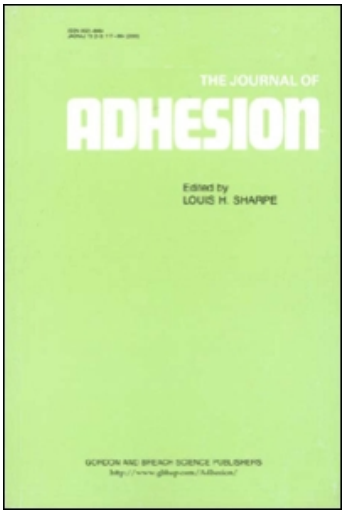

The Journal of Adhesion

Publication details, including instructions for authors and subscription information:
http://www.informaworld.com/smpp/title~content=t713453635

Similarity Concepts in the Fatigue Fracture of Adhesively Bonded Joints

C. Lin[a]; K. M. Liechti[a]
[a] Engineering Mechanics Research Laboratory, Department of Aerospace Engineering and Engineering Mechanics, The University of Texas at Austin, Austin, Texas, U.S.A.

To cite this Article Lin, C. and Liechti, K. M.(1987) 'Similarity Concepts in the Fatigue Fracture of Adhesively Bonded Joints', The Journal of Adhesion, 21: 1, 1 — 24
To link to this Article: DOI: 10.1080/00218468708074956
URL: http://dx.doi.org/10.1080/00218468708074956

J. Adhesion, 1987, Vol. 21, pp. 1–24
Photocopying permitted by license only

Printed in the United Kingdom

Similarity Concepts in the Fatigue Fracture of Adhesively Bonded Joints†

C. LIN and K. M. LIECHTI

Engineering Mechanics Research Laboratory, Department of Aerospace Engineering and Engineering Mechanics, The University of Texas at Austin, Austin, Texas 78712, U.S.A.

(Received October 22, 1985; in final form April 15, 1986)

Cyclic debond data obtained from fatigue testing of four different specimen geometries having the same adhesive is considered. Fatigue properties of the adhesive are characterized in terms of linear elastic fracture mechanics concepts whereby debond growth rates are correlated to appropriate mixed mode fracture parameters. Stress analyses of the four specimens under maximum load indicate that in most cases inclusion of geometric nonlinearities is required for the determination of the fracture parameters. For three of the specimens considered, the debond growth laws based on total energy release rate as correlating mixed-mode fracture parameter were found to be similar. A number of potential reasons for the lack of similarity in debond growth laws in all four specimens are explored.

KEY WORDS Adhesive joints; cyclic debonding; damage tolerant design; finite element stress analysis; geometric nonlinearity; mixed mode fracture.

INTRODUCTION

Recent improvements in adhesive materials and adhered surface preparations have increased the feasibility of adhesive bonding in primary structural applications. In view of the long term nature of many applications questions of bond durability must therefore be addressed. One particularly important aspect of bond durability

† Presented at the Ninth Annual Meeting of The Adhesion Society, Inc., Hilton Head Island, SC, U.S.A., February 9–12, 1986.

considerations arises due to the cyclic nature of many practical structural loadings. In many cases crack growth due to cyclic loading may occur at load levels that are much lower than those that are predicted on the basis of noncyclic or static loads. The potential for cyclic debonding in adhesively bonded joints must therefore be assessed with a view either to establishing threshold load levels (for infinite life designs) or to predicting debond growth histories (finite life designs). The problem of fatigue crack growth in adhesively bonded joints was first addressed by Mostoroy and Ripling[1] under opening mode fracture conditions and then later, under mixed mode fracture conditions by Marceau *et al.*[2] and Brussat *et al.*[3] In these early studies the adhesive thickness was treated as a microstructual property and analyses were conducted on the basis of the stresses and strains in the adherends. The adhesive layer then defined the crack path and the fracture mechanics concepts that had been developed for monolithic materials were then used to characterize the debonding of adhesively bonded joints. Correlations between debond growth rates and the change in fracture parameter over one load cycle resulted in the same sigmoidal shapes that had been previously observed in studies of fatigue crack propagation in metals. For values of fracture parameter above certain threshold values and below the fracture toughness of the adhesive, simple crack growth laws following the familiar power law of the type first suggested by Paris were used to characterize the fatigue properties of the adhesive. The mixed mode character of debonding was reflected in the variety of fracture parameters that were used in making the crack growth rate correlations. Effects of temperature and moisture[2] and crack closure[4] (under mode I conditions) were also considered.

The importance of including the adhesive layer in stress and fracture analyses of adhesively bonded joints was first stressed by Wang *et al.*[5] More recent fatigue studies[6–13] have also considered the adhesive layer as a macrodimension that is included in the analysis. Such an approach allows for variations in debond location (adhesive or cohesive) to be considered and had the potential for including the effects of nonlinearity in the constitutive behavior of the adhesive and its sensitivity to the effects of and time, temperature and moisture.[12] Fracture parameters are calculated on the basis of the local stresses and displacements in the material in which the

debond is propagating and most of the more recent studies have been directed towards the determination of a unifying mixed mode fracture parameter that governs cyclic debonding under all conditions. For example, after Dattaguru *et al.*[6] had demonstrated the importance of including geometrical nonlinearities in the analysis of the cracked lap shear specimens that were used to develop mixed mode fracture data; studies by Everett[7] that involved localized clamping of cracked lap shear specimens indicated that mode I energy release rates governed cyclic debonding rates. The specimens that were used[7] were made up of graphite epoxy bonded to aluminum with EA-934. However, in subsequent studies by Mall *et al.*,[8,9] involving cracked lap shear and double cantilever beam specimens made of all-composite adherends and ED-3445 and FM-300 adhesives, it was found that debond growth rates correlated best with the total energy release rate. At the same time, Romanko *et al.*[10,11] considered a number of specimen geometries in which aluminum adherends were joined by FM-73M. The joints were tested over a range of frequencies, temperatures and moisture contents. However, the correlations between debond rates and fracture parameters that were made[11] were based on relatively limited stress analyses, pending the development of the finite element code VISTA[12] that is capable of viscoelastic and geometrically nonlinear analysis.

In the present work, VISTA has therefore been used to conduct a consistent series of stress analyses of four of the specimen geometries that were subjected to fatigue testing in Refs 10 and 11. Growth laws for cyclic debonding under room temperature environments have been established which allow similarity concepts, the basis of predictions of joint durability, to be evaluated over a range of mixed mode fracture conditions. In what follows, the four specimen geometries are first described with reference to the nature and history of the debonding that was observed. On the basis of the maximum loads that each type of specimen encountered in the testing program, the effects of large deflections on energy release rates are then considered by comparing the results of linear and geometrically nonlinear analyses. The ranges of total energy release rate and ratio of opening to shear modes that arose in the four specimens are also compared prior to the determination of debond growth laws and the ensuing discussion.

SPECIMEN GEOMETRIES

A total of five specimens were analysed in this study. Four of the specimens were used in the fatigue crack growth studies and the fifth was used to validate VISTA, the finite element code that was employed throughout the work for stress analysis. The four fatigue crack growth specimens were all made of bare aluminum alloy 7075-T651 adherends and FM-73M adhesive.† The adherends were alkaline cleaned, acid etched and phosphoric-acid anodized using the BAC-5555 process. After oven drying following the rinse, the anodized parts were coated with Bloomingdale BR127 primer and cured for 30 minutes at room temperature followed by a 60 minute soak at 250°F. The adhesive is a 250°F cure tape having a matte Dacron® carrier. The geometric details of the specimens that are described here are those that were employed in the stress analysis of the joints. The finite element models do not include the details of specimen gripping arrangments such as bolt hole locations and the reader will therefore be referred to the original reports for such details.

† Made available for these studies by American Cyanamid, Havre de Grace, MD, U.S.A.

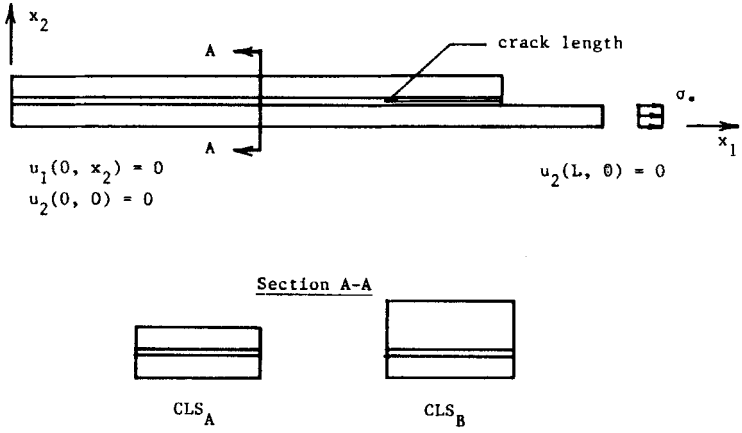

FIGURE 1 ASTM round robin cracked lap shear specimen (CLS).

The geometry of the specimen that was used for mesh refinement studies is shown in Figure 1. It is a version of the cracked lap shear specimen that has been used in a number of studies[6,9] and is the subject of a recent ASTM Round Robin Analysis.[13] The two adherends are fixed at the left hand end ($x_1 = 0$) and the load is applied to the other end of the longer (strap) adherend. Two configurations, CLS_A and CLS_B, and various lengths of cohesive crack emanating from the free edge of the adhesive layer were considered. The specific dimensions of the adherends and adhesive layer of this and all other specimens are summarized in Table I.

The first of the fatigue crack growth specimens that was considered is the model thick-adherend single lap shear specimen, or model joint (MJ). The geometry that was modeled in the finite element analysis is shown in Figure 2 and represents an antisymmetric half of the joint. Details of the full joint and its bolt hole locations are shown in Figure 1 of Ref. 10. Cracks of equal length emanated either cohesively or adhesively from the two bond terminations. Antisymmetric boundary conditions were employed along $x_1 = 0$, the plane of antisymmetry, with a uniform traction being applied at $x_1 = L$.

The second and third fatigue crack growth specimens that were employed in this study belonged to the cracked lap shear specimen (CLS) family (Figure 3) that was originally proposed by Brussat *et al.*[3] Differing relative amounts of mode I and mode II can be obtained depending on the relative thicknesses of the strap (directly loaded) and lap adherends. Thus in Figure 3 it can be seen that in the CLS_1 specimen the strap adherend is thicker than the lap adherend, whereas in the CLS_2 specimen the situation is reversed. Both specimens were side-grooved to ensure that cracks grew in the adhesive. The full joint geometries are shown in Figure 6 of Ref. 11. The loads were introduced to the specimens through a clevis arrangement that allowed the joints to rotate at the ends. The joint was therefore considered to rotate about the mid thickness of the two adherends at $x_1 = 0$, and the mid thickness of the strap adherend at $x_1 = L$, with a uniform traction being applied at $x_1 = L$. Cracks were introduced to the specimen in a precracking schedule that involved gradually decreasing loads to produce initial cohesive crack lengths on the order of 75 mm.

The last fatigue crack growth specimen to be considered here was

TABLE I
Specimen dimensions, properties and tractions

	CLS_A	CLS_B	MJ	CLS_1	CLS_2	SLJ
Upper adherend length (m)	0.254	0.254	0.062*	0.483	0.483	0.076†
Lower adherend length (mm)	0.305	0.305	0.062*	0.559	0.559	0.206†
Overlap length (m)	0.254	0.254	6.35 mm	0.483	0.483	0.073
Upper adherend thickness (mm)	3.175	6.35	6.35	9.525	19.05	3.175
Lower adherend thickness (mm)	3.175	3.175	6.35	19.05	9.525	3.175
Adhesive thickness (mm)	0.127	0.127	0.254	0.254	0.254	0.254
Width (mm)	25.4	25.4	25.4	5.08‡	5.08‡	152.4
Adhesive modulus (GPa)	1.93	1.93	2.07	2.07	2.07	2.07
Adhesive Poisson ratio	0.4	0.4	0.32	0.32	0.32	0.32
Traction σ_0 (MPa)	137.80	137.80	20.7	411.3	414.1	229.8

Adherend modulus = 72.4 GPa, adherend Poisson ratio = 0.33.
* Antisymmetric analysis, length listed is the specimen half-length.
† Symmetric analysis, length listed is the specimen half-length.
‡ Notched width.

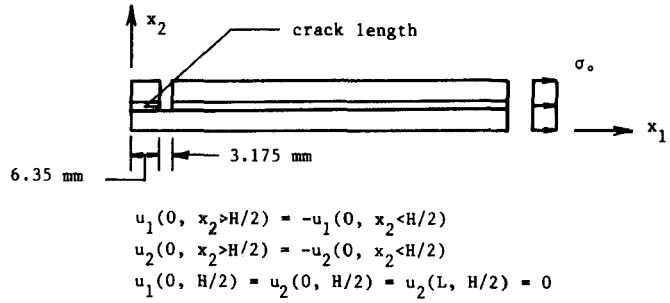

FIGURE 2 Mode thick-adherend single lap shear specimen (MJ).

the structural single lap strap joint (SLJ) that was originally proposed by Brussat *et al.*[3] Due to symmetries in the specimen and the crack growth histories, only half the specimen was modeled (Figure 4) with the plane of symmetry being taken along $x_2 = 0$. The full geometry of the specimen is shown in Figure 7 of Ref. 11. Cracks emanated from the center of the joint and grew in a cohesive manner towards the edges of the bondline that coincided with the lap terminations.

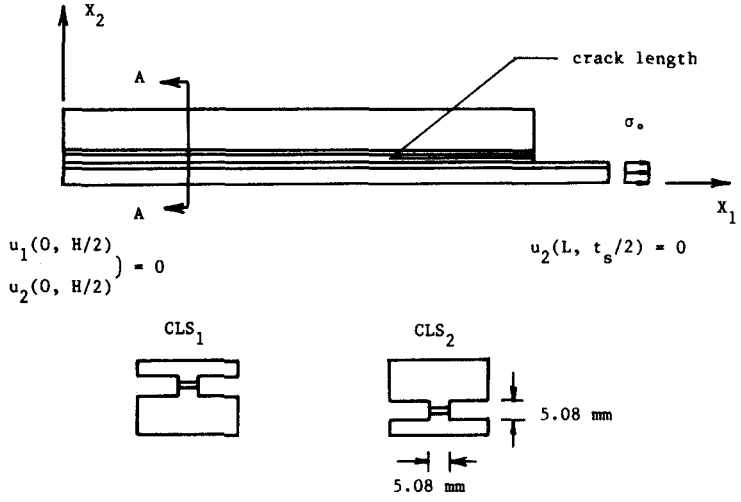

FIGURE 3 Cracked lap shear specimen.

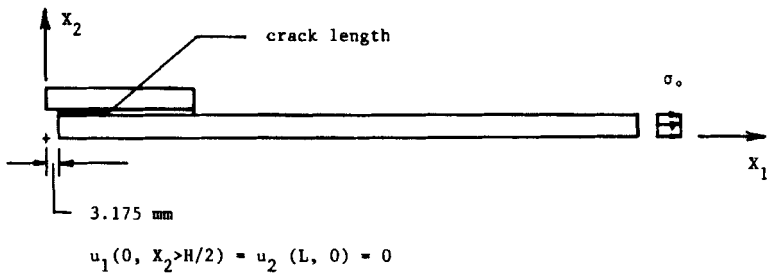

FIGURE 4 Structural single lap strap joint.

DEBOND HISTORIES

The debond histories of the four specimens are summarized in Figure 5. In the model joint, debonds emanated from the bond termination at $x_1 = 6.35$ mm and grew adhesively and cohesively towards $x_1 = 0$. Because of the relatively small dimensions of the overlap, ultransonic methods of crack length measurement could not be employed. In the data considered here, the extent of debonding was measured by etching away the adherends after a given number of cycles. Thus a number of specimens, cut from the same location of a large bonded plate, were used to generate the single curve shown in Figure 5. Crack lengths in the cracked lap shear specimens were measured ultrasonically. The crack growth histories reflect the fact that the applied loads were increased roughly every 40 mm to provide a wider range of energy release rates per specimen. In the structural lap joints, crack front locations were also measured ultrasonically. Cracks grew in a symmetric fashion with crack fronts that were quite linear across the width. Slight deviations in crack symmetry and crack front linearity were averaged out in the crack growth data (obtained at three different load levels) that are recorded in Figure 5.

STRESS ANALYSIS

The finite element code VISTA, developed by Becker *et al.*,[12] was used to conduct stress analyses of the various joints considered in

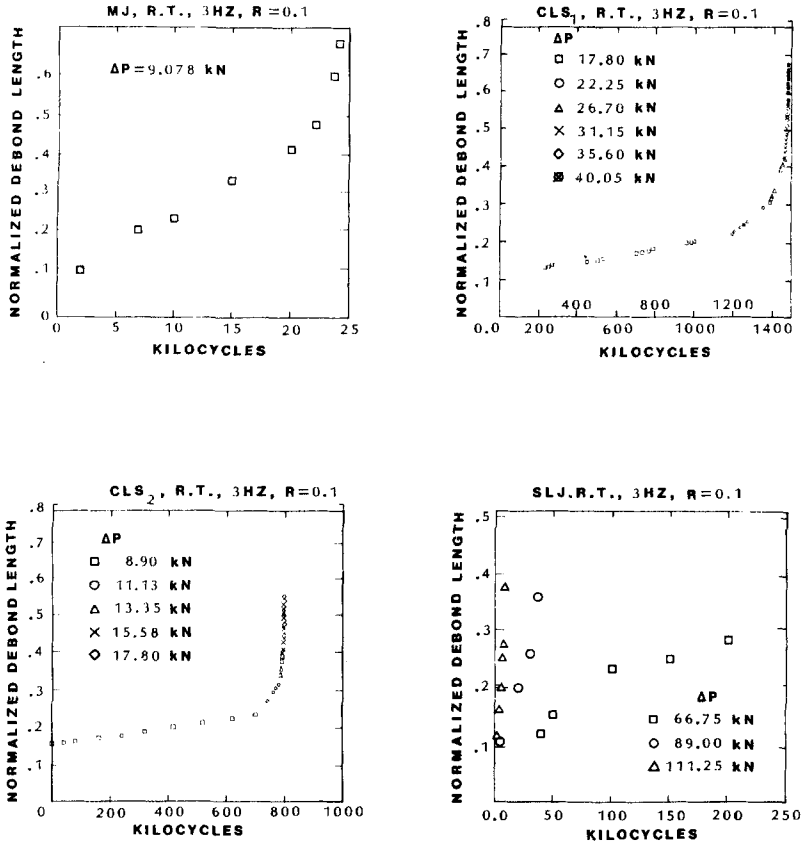

FIGURE 5 Debond growth histories.

this study. The adherends and adhesive were considered to be linearly elastic, isotropic materials having the mechanical properties noted in Table I. A plane strain analysis was conducted using isoparametric, quadratic quadrilateral elements in regions removed from the crack tip. The singular strains in the crack tip region were captured by a variable singularity, six node triangular element that also incorporates a constant strain field.[14] Another feature of VISTA that was useful in the present study was the ability to conduct geometrically nonlinear analyses and thereby account for

the large deflections that were observed during the testing of some of the specimens.

Calculation of fracture parameters

The fracture parameters that were calculated from the solutions were the total energy release rate G and its components G_I and G_{II}, the opening and shear mode energy release rates respectively. In the singular element, along any ray emanating from the crack tip, the displacements u_α, that give rise to the singular strains and stresses are expressed in the form

$$u_\alpha = C_\alpha r^\lambda, \quad \alpha = 1, 2 \tag{1}$$

The eigenvalue λ may be chosen to reflect any type of singularity and the displacement coefficients C_α are then obtained directly from the solution along rays corresponding to the sides of the triangular elements surrounding the crack tip. In this study, energy release rates were calculated on the basis of the displacements of the element sides corresponding to the crack faces. If these displacements are characterized by the coefficients C_α^+ and C_α^- for the upper and lower crack faces, respectively, then G_I and G_{II} for cohesive cracks may be obtained in the form

$$G_I = \frac{\pi E}{32(1-\nu^2)}(\Delta C_2)^2 \tag{2}$$

$$G_{II} = \frac{\pi E}{32(1-\nu^2)}(\Delta C_1)^2 \tag{3}$$

where $\Delta C_\alpha = C_\alpha^+ - C_\alpha^-$. The total energy release rate, G, is then obtained by the addition of G_I and G_{II}.

The determination of linear elastic fracture parameters for interface cracks is complicated by the oscillatory singularities in the normal and shear stress and strains that are predicted by linear analyses. The resulting bimaterial stress intensity factors K_1 and K_{II} are functions of an arbitrary length scale and are therefore not suitable for use as fracture parameters or criteria. However, when the total energy release rate or the overall[14] and interfacial[15] stress intensity factors are considered [all of which involve $(K_I^2 + K_{II}^2)$], the arbitrary length scale drops out because it is embedded in trigono-

metric terms which become unity when K_I and K_{II} are squared and summed. In Ref. 16, Smelser established the equivalence between the J-integral and overall stress intensity factor for interface cracks between bimaterial bodies. The magnitude of the vectorial crack opening displacement was also given in terms of the overall stress intensity factor. Thus if we bear in mind the equivalence between the J-integral and the energy release for linearly elastic materials and make use of Eq. (1), the energy release rate may be expressed in terms of the displacement coefficients that are output from VISTA

$$G = \frac{2\pi\lambda_0^2}{(\Lambda_1 + \Lambda_2)}[\Delta C_1^2 + \Delta C_2^2] \tag{4}$$

where

$$\lambda_0 = \tfrac{1}{2}(1 + 4\varepsilon^2)^{1/2}$$

$$\varepsilon = \frac{1}{2\pi} \ln \frac{\mu_1 + \mu_2 k_1}{\mu_2 + \mu_1 k_2}$$

and $\Lambda_\alpha = 4(1 - \nu_\alpha)/\mu_\alpha, \quad \alpha = 1, 2$

In examining mixed mode effects, G_I was associated with the component of crack opening displacement normal to the interface (represented by ΔC_1) whereas G_{II} was associated with the component of crack opening displacement parallel to the interface (represented by ΔC_2).

Mesh refinement

In the past, the main difficulties that have arisen in the application of finite element methods to the bonding problem have been due to the thinness of the adhesive layer and the large variation in adhesive and adherend moduli. These difficulties may be expected to be even more severe when cracks are present in the adhesive layer. The singular elements used in VISTA are intended to capture the square root singular behavior in stresses and strains. It is to be expected that the square root behavior will dominate over a certain distance from the crack tip with higher order terms contributing more strongly at larger distances from the crack tip. In order to model the crack in an optimum manner, the size of the singular elements should be chosen to be the same size as the region of square root

dominance. The first step in the present work therefore involved a grid optimization phase in which the solutions that were obtained using various mesh sizes in the crack tip region were compared with existing solutions.

The problem that was chosen for the mesh refinement study was the ASTM Round Robin Cracked Lap Shear Specimen depicted in Figure 1. The first level of refinement that was considered was a mesh that contained four equal layers of elements through the adhesive thickness. In the crack tip region the aspect ratio of element length to height of the elements was exactly one and was gradually increased at larger distances from the crack tip. A number of crack lengths in the CLS_A and CLS_B specimens were considered and the resulting variation in energy release rate is shown in Figure 6. The results, designated CLS_A and CLS_B COARSE, are compared with solutions that were obtained analytically and using other finite element codes.[13] For shorter debond lengths, the coarse mesh results were greater than the benchmark solutions by as much as 40%. Much closer agreement is apparent for normalized, debond lengths on the order of 0.4. The mesh in the adhesive was then refined, still keeping four elements through the thickness, but with the two central layers of elements accounting for less than half of the adhesive thickness, t_a. Best agreement was obtained when the two central layers occupied $0.052t_a$ as indicated by the CLS_A and CLS_B FINE results that are shown in Figure 6. The same basic mesh in the region surrounding the crack tip was therefore used in all subsequent analyses.

Geometrically nonlinear effects

During the testing of the four fatigue specimens it was observed that in some cases certain combinations of load levels and crack lengths resulted in relatively large joint deflections. Furthermore, even in the case of the end-clamped cracked lap shear specimen (a relatively stiff arrangement), Dattaguru *et al.*[6] showed that energy release rates were reduced significantly when geometrically nonlinear effects were included in the analysis. In view of these observations, geometrically nonlinear analyses of the four fatigue specimens were therefore conducted. The analyses were performed over a full range of crack lengths in each specimen. The load levels

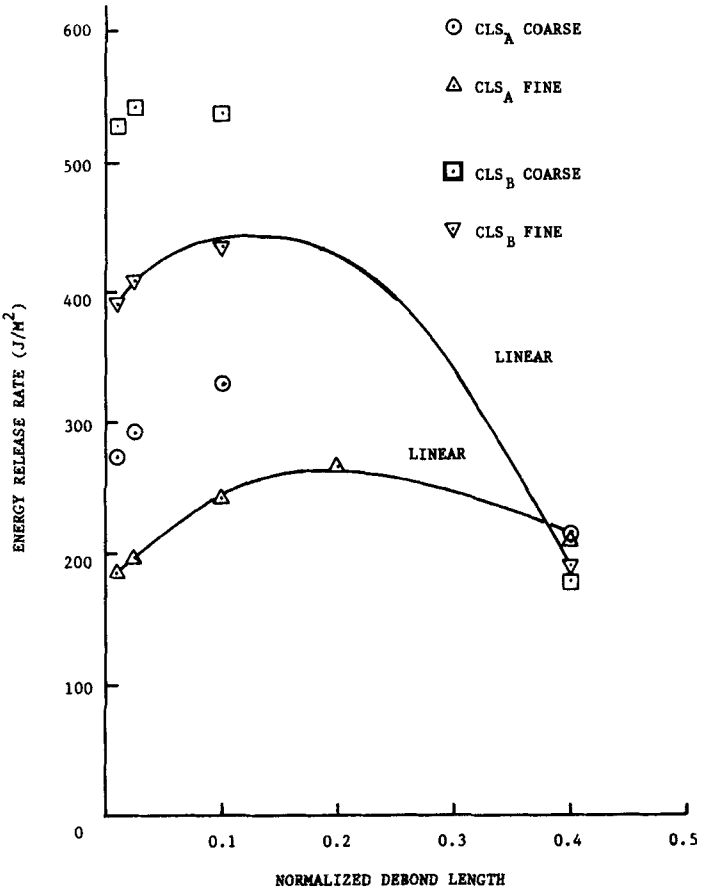

FIGURE 6 Vista mesh refinement study.

that were used in the analyses were the maximum loads encountered in the testing and are recorded in Table I. Since these load levels resulted in nominally similar crack growth rates in all joints, the results will also be useful later in examining similarity concepts. In what follows, detailed results are presented for each specimen in individual plots where geometrically nonlinear effects are examined. With an appropriate level of analysis thus defined, an overall picture of the range of energy release rates and ratios of shear to opening mode energy rates in the four specimens is then presented.

The model joint under an applied traction of 20.7 MPa was analyzed for a range of normalized debond lengths up to 60%. The general pattern of debonding in the model joints was that of an initial adhesive debond followed by cohesive (and usually catastrophic crack growth) since the relative amounts of adhesive and cohesive debonding were not identified,[10] both possibilities were analyzed here. For the linear analyses it can be seen (Figure 7) that although G_I and G_{II} show some dependence on debond location through the thickness, the total energy release, G, is relatively insensitive to debond location. A geometrically nonlinear analysis was therefore only conducted for the case of a cohesive debond. The lack of difference in G_I and the small differences in G_{II} and therefore G between the linear and nonlinear analysis indicate that large deflections do not occur in this specimen geometry due to the relatively thick adherends. It is also interesting to note that the mode I component decreases with increasing debond length to

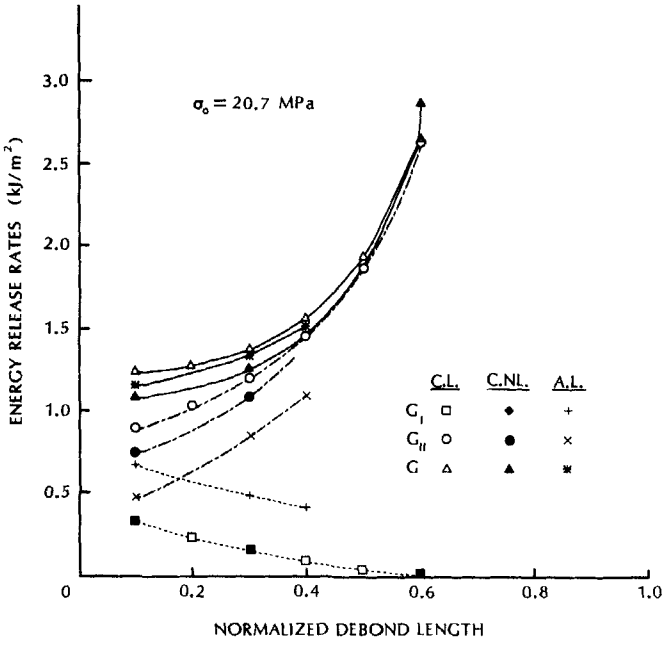

FIGURE 7 Energy release rates for model joint (MJ).

make the specimen a pure mode II specimen for normalised debond lengths greater than 0.6.

The applied traction that was considered in the analysis of the CLS_1 and CLS_2 specimens was 411.3 and 414.1 MPa, respectively. The value of the applied traction was obtained by dividing the applied load by the thickness of the strap adherend and the width of the notched region (5.08 mm). The extra width of the unnotched portions of the adherends was accounted for by increasing the modulus in the unnotched region by a factor of 5, the ratio of the width of unnotched to the width of the notched region.

The variation in energy release rates with normalized debond length for the GLS_1, specimen is shown in Figure 8. The results indicate that G_{II} was always greater than G_I and that the consideration of geometrically nonlinear effects led to decreases in G_I and especially G_{II}, particularly for the longer debonds. For the range of normalized debond lengths that were considered, G was reduced by

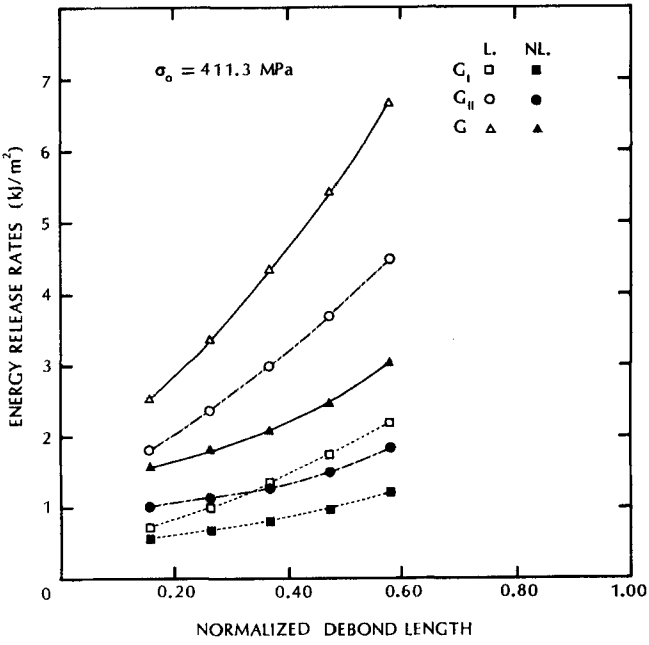

FIGURE 8 Energy release rates for CLS_1 specimen.,

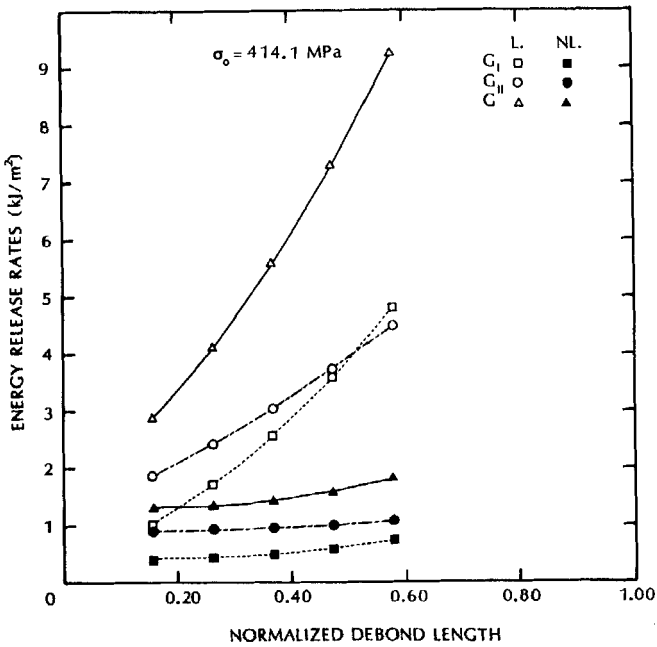

FIGURE 9 Energy release rates for CLS_2 specimen.

approximately a factor of 2 when large deflections were accounted for.

Similar trends can be observed in the results (Figure 9) for the CLS_2 specimen. However, the effects of geometrical nonlinearity on energy release rates were stronger than in the case of the CLS_1 specimen and more evenly distributed between G_I and G_{II}. G was reduced by as much as a factor of 5 in the nonlinear analysis.

The applied traction that was considered in the analysis of the structural lap joint was 229.83 MPa. The mode I and mode II contributions to the energy release rate were almost equal (Figure 10) and, particularly under a linear analysis, were essentially independent of debond length. Consideration of geometrically nonlinear effects resulted in a dramatic decrease (more than a factor of 10) in energy release rates and a change from mode I dominance to mode II dominance. A greater variation in energy release rates with debond length was also observed.

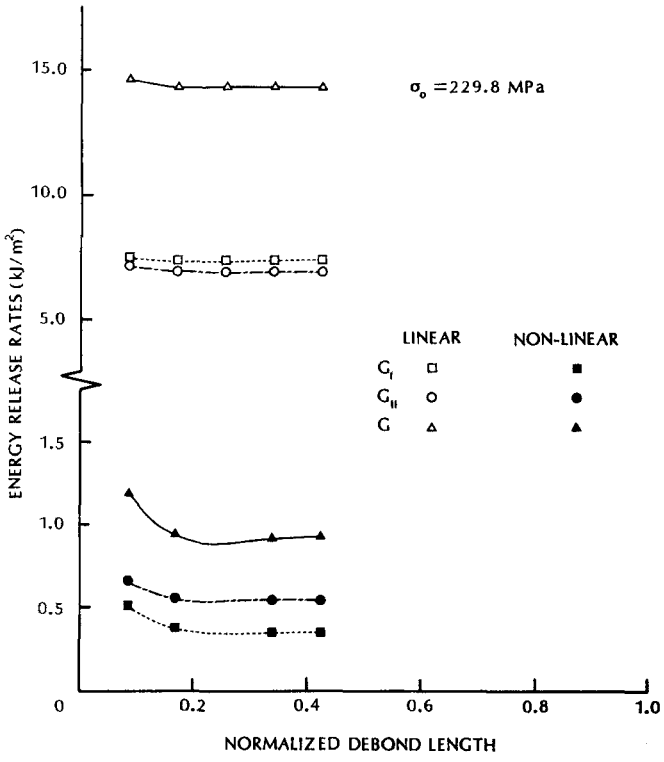

FIGURE 10 Energy release rates for structural lap joint (SLJ).

To summarize, the results depicted in Figures 7–10 indicate that geometrically nonlinear analyses resulted in substantial decreases in energy release rates in all specimens except the model joint. The ranges of energy release rates that were produced in the various specimens, under the maximum load amplitude that was used in testing are summarized in Figure 11. Since only one load amplitude was used in the testing of the model joint, the range of energy release rates shown in Figure 10 reflects the full range encountered during testing. In the other specimens, the full range encountered was actually greater because a number of lower load amplitudes were employed in the testing. Nevertheless, it is clear that the severity of the energy release rates was greatest in the CLS_I

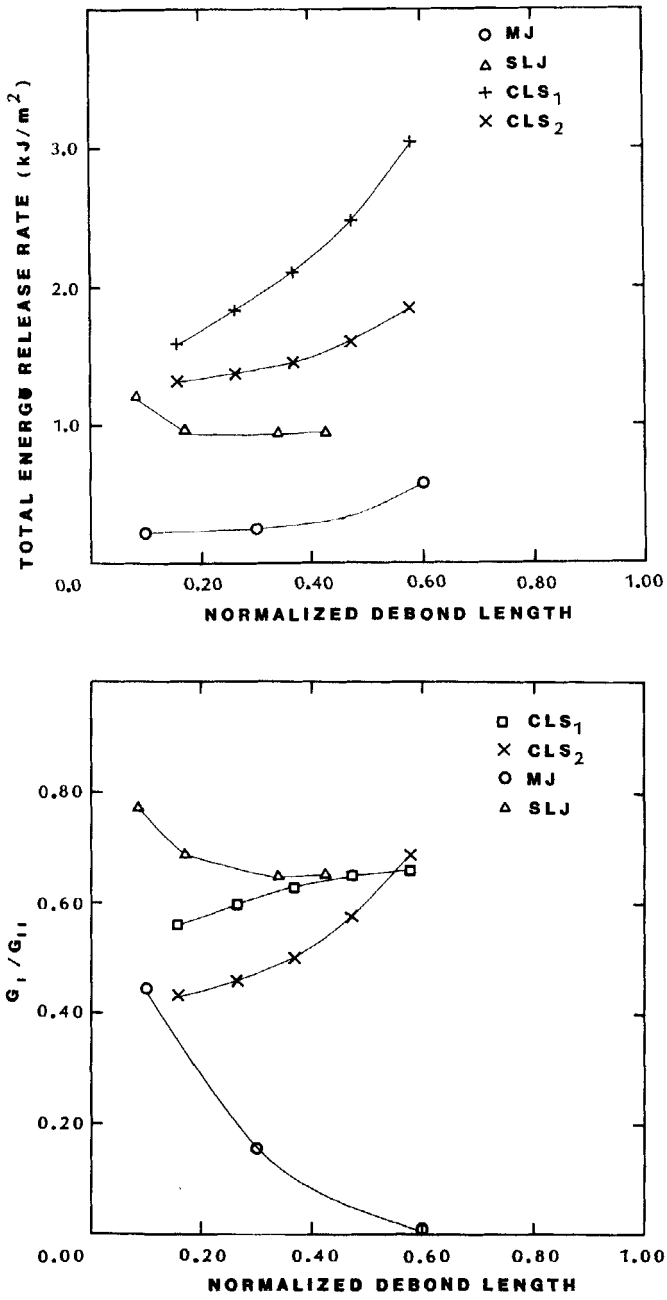

FIGURE 11 Comparison of energy release rates in all fatigue specimens.

specimen, followed by the CLS_2 specimen, the structural lap joint and the model joint. In view of the mixed mode nature of debonding in these specimens, the ratio of G_I/G_{II} predicted by geometrically non-linear analyses are also shown in Figure 11. The maximum load used in the testing of the specimens is again used as the basis for the comparison. The specimen with by far the highest mode II content is the model joint, followed by the CLS_2, CLS_1 and structural lap joint with some overlap between the later two at the longer debond lengths.

CORRELATION OF DEBOND GROWTH RATES

The debond growth rates that were measured in the testing program were above threshold values in that cyclic debonding occurred and below critical values in that catastrophic failure only occurred after an extended period of subcritical cyclic debonding. Correlations between debond growth rates (da/dN) and change in mixed-mode fracture parameter (or driving force) over one load cycle (ΔP) were therefore sought which had the form

$$da/dN = A(\Delta P)^n \tag{5}$$

where A and n can be thought of as material properties that characterize the fatigue behavior of the adhesive. In view of the relative toughness of FM-73M, the mixed-mode fracture parameter that was chosen as the basis of discussion in making debond growth rate correlations was the toal energy release rate, G. In view of the importance of nonlinear effects considered earlier, values of ΔG were obtained directly from finite element analyses of each separate load level and range of debond lengths.

The correlations between growth rates and ΔG for the four specimens are shown in Figure 12. The lines drawn through the data reflect the best linear fit between $\log(da/dN)$ and $\log(\Delta G)$ in a least squares sense. The corresponding values of A and n in (5) are shown in Table II, along with the correlation coefficient r. It can be seen that the best agreement between the correlations occurs between the data that were obtained from the testing of the model joint and the structural lap joint. The slope of line obtained from the correlations of the CLS_2 data is also in reasonable agreement

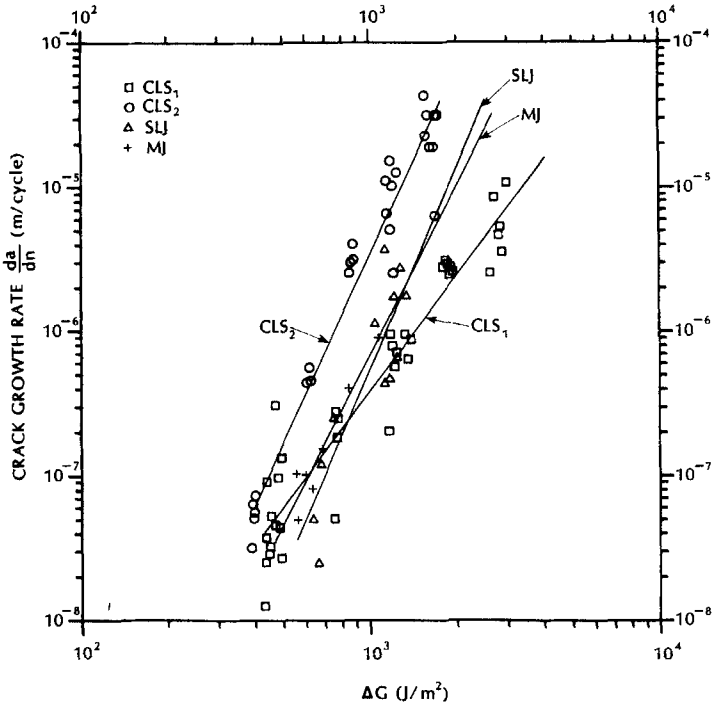

FIGURE 12 Debond growth rate correlations.

although for the given values of ΔG, the CLS_2 debond growth rates area consistently higher than those of the model and structural lap joints by factors of 5 to 8. Such a spread in fatigue data is often acceptable but the fact that the difference between the two sets of data is not random may be indicative of a consistent trend. The most notable lack of similarity between the four data sets arises from the correlations obtained from the CLS_1 specimen. The slope

TABLE II
Correlation of debond growth rates with energy release rate

	MJ	CLS1	CLS2	SLJ
Exponent	3.99	2.69	4.30	4.86
Intercept	7.2E-19	3.3E-15	4.3E-19	1.3E-21
Correlation coefficient	0.963	9.954	0.978	0.880

of the best fit line is much lower than any of the others, and, over the range of energy release rates considered, the debond growth rates in the CLS_1 tests were less than those of the CLS_2 specimen by factors of 2 to 25.

The cracked lap shear specimens were recently the subject of a repeatability study[17] in which identical specimens were tested under exactly the same conditions as the CLS_1 and CLS_2 specimens[11] that were the subject of this work. The debond growth rate correlations that were made on the basis of new tests in[17] are compared with the current work in Figure 13. It can be seen that the two sets of CLS_1 data are in close agreement which would seem to indicate that the deviation of the CLS_1 data is at least consistent. However, the two ses of CLS_2 data are noticeably different with the debond growth rates measured in[17] being consistently greater for a given value of ΔG. The lack of agreement may be partly due to a difference in the

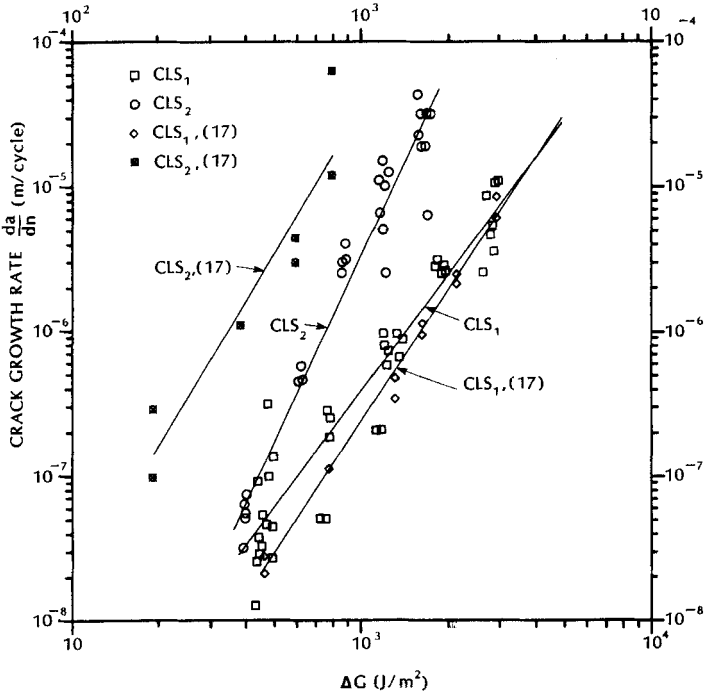

FIGURE 13 Repeatability of cracked lap shear data.

dependence of energy release on debond length that was predicted by the two analyses: In Ref. 17, there was a local maximum in the function relating energy release rates to debond length whereas the results of the present study (Figure 9) indicate a monotonically increasing dependence.

At this stage, it therefore appears that similarity concepts based on linear elastic fracture mechanics concepts may be applicable. The main exception is in the case of the CLS_1 specimen and the question therefore arises as to the possible causes of the noted difference. The first possibility is the uncertainty that is introduced in the cracked lap shear data by the way that the specimens are loaded. The loads are introduced by a double clevis arrangement [Ref. 17, Figure 4] which is supposed to allow for free rotation of the specimen ends. Frictional effects and other uncertainties[17] may not in fact provide the free rotation condition that was modeled in the finite element analysis. For example, the eccentricity in the load path that drives the rotation is smaller in the CLS_1 specimen and may not always be high enough to overcome frictional effects. Furthermore, energy release rates have been found to be quite sensitive to slight changes in end conditions. The second possible cause of lack of similarity may be due to inappropriate choice of mixed mode fracture parameter. However, this possibility is unlikely because of the good agreement between the data from the model and structural lap joints, which represented opposite ends of the G_I/G_{II} spectrum that was investigated. Finally, the only remaining aspect that has not been considered analytically is the extent of nonlinear behavior of the material in the crack front region. At first sight, this possibility looks encouraging because the driving force or level of energy release rate was highest for the CLS_1, specimen. It might therefore be argued that, for a given G, debond growth rates would be lower due to plasticity effects such as crack closure. However, this would not explain why the crack growth rates were highest in the CLS_2 specimen which was subjected to the second largest level of driving force.

CONCLUSIONS

Cyclic debonding data from four different joints having the same adhesive has been examined. Stress analyses of the various con-

figurations of load levels and geometries that arose in the testing were conducted. Geometrical nonlinearities were included in the analyses and strongly influenced the energy release rates in all specimens except the model joint. Energy release rates or driving forces applied to the specimens ranged from 0.4 to 3 kJ/m^2 with G_I/G_{II} ratios ranging from 0 to 0.8. Correlations between debond growth rates and the total energy release rate as mixed mode fracture parameters were examined. Two of the data sets were in very close agreement while a third data set exhibited a notable shift that was, however, still within accepted scatter bounds for fatigue data. However, a noticeable difference between these three data sets and the fourth indicates the potential for configurational dependence in debond growth rate correlations. Factors that were considered to be the most likely cause of the lack of similarity included the appropriate modeling of end conditions in the cracked lap shear specimens and the extent of material nonlinear behavior in the crack front region. Since the two data sets exhibiting the closest agreement came from specimens having the lowest and highest G_I/G_{II}, it is clear that the mode I energy release rate does not control cyclic debonding in the relatively tough adhesive considered here.

In view of the sensitivity of energy release rates to slight changes in boundary conditions, the use of the clamped version of the cracked lap shear specimen[13] is recommended. All calculations of energy release rates were made solely on the basis of numerical stress analyses. Because of the large effect of geometric nonlinearity and the potential for material nonlinearity it is also recommended that numerically calculated fracture parameters be compared to those obtained on the basis of experimental stress analyses. Measurements of local crack tip displacement fields would also permit crack closure effects to be examined.

Acknowledgements

This work was made possible by the careful planning and foresight of Professor W. B. Jones (currently at Texas Technical University, Lubbock) who was the Air Force Project Engineer of the programs whose results are reported in Refs 10–12. The contributions of Dr. J. Romanko and Professors W. G. Knauss and E. B. Becker in developing the data base and analytical tools that formed the basis for this work are also gratefully acknowledged. Many thanks are also due to Ms. Mariou Barr for timely preparation of the manuscript.

References

1. S. Mostovoy and E. J. Ripling in Adhesion Science and Technology **Vol. 9B** (Plenum Press, N.Y., 1975), pp. 513–562.
2. J. A. Marceau, J. C. McMillan and W. M. Scardino "Cyclic Testing of Adhesive Bonds; SAMPE 22nd Nation SAMPE Symposium and Exhibition, **22** (1977), pp. 64–80.
3. T. R. Brussat and S. T. Chiu, *J. Eng. Mat. and Tech.* **100,** 39–45 (1978).
4. D. A. Jablonski, *J. Adhesion* **11,** 125–143 (1980).
5. S. S. Wang and J. F. Yau, *Int. J. Fracture* **19,** 295–309 (1982).
6. B. Dattaguru, R. A. Everett, Jr., J. D. Whitcomb and W. S. Johnson, *J. Eng. Mat. and Tech.* **104,** 59–65 (1984).
7. R. A. Everett, Jr., *Adhesives Age* **26,** 24–29 (1983).
8. S. Mall, W. S. Johnson and R. A. Everett, Jr., "Cyclic Debonding of Adhesively Bonded Composites", NASA TM-84577, November 1982.
9. S. Mall and W. S. Johnson, "Characterization of Mode I and Mixed-Mode Failure of Adhesive Bonds Between Composite Adherends", NASA TM 86355, February 1985.
10. J. Romanko and W. G. Knauss, "Fatigue Behavior of Adhesively Bonded Joints" AFWAL-TR-80-4037, April, 1980.
11. J. Romanko, K. M. Liechti and W. G. Knauss, "Integrated Methodology for Adhesive Bonded Joint Life Predictions" AFWAL-TR-82-4139, November, 1982.
12. E. B. Becker, R. S. Chambers, L. R. Collins, W. G. Knauss, K. M. Liechti and J. Romanko, "Viscoelastic Stress Analysis of Adhesively Bonded Joint Including Moisture Diffusion". AFWAL-TR-84-4057, August, 1984.
13. W. S. Johnson, "Stress Analysis of the Cracked Lap Shear Specimen: An ASTM Round Robin" To be published in *J. of Testing and Evaluation.*
14. M. Stern, *Int. J. for Numerical Methods in Eng.* **14,** 409–421 (1979).
15. S. G. Sawyer and R. B. Anderson, *Eng. Fract. Mech.* **4,** 605–616 (1972).
16. R. E. Smelser and M. E. Gurtin, *Int. J. Fracture* **13,** 382–384 (1977).
17. R. A. Everett and W. S. Johnson, in *Delamination and Debonding of Materials,* ASTM STP 876 (American Society for Testing and Materials, Philadelphia, 1985).